

Lawrence Berkeley National Laboratory

Recent Work

Title

EXPERIMENTAL TEST OF THE $A_S=A_Q$ RULE IN LEPTONIC DECAYS OF NEUTRAL K MESONS

Permalink

<https://escholarship.org/uc/item/5gw9c0cv>

Authors

Webber, Bryan R.
Solmitz, Frank T
Crawford, Franks.
et al.

Publication Date

1970-06-01

c. 2

EXPERIMENTAL TEST OF THE $\Delta S = \Delta Q$ RULE IN
LEPTONIC DECAYS OF NEUTRAL K MESONS

Bryan R. Webber, Frank T. Solmitz,
Frank S. Crawford, Jr., and Margaret Alston-Garnjost

June 1970

AEC Contract No. W-7405-eng-48

RECEIVED
LAWRENCE
RADIATION LABORATORY

SEP 30 1970

LIBRARY AND
DOCUMENTS SECTION

TWO-WEEK LOAN COPY

*This is a Library Circulating Copy
which may be borrowed for two weeks.
For a personal retention copy, call
Tech. Info. Division, Ext. 5545*

LAWRENCE RADIATION LABORATORY
UNIVERSITY of CALIFORNIA BERKELEY

c. 2

DISCLAIMER

This document was prepared as an account of work sponsored by the United States Government. While this document is believed to contain correct information, neither the United States Government nor any agency thereof, nor the Regents of the University of California, nor any of their employees, makes any warranty, express or implied, or assumes any legal responsibility for the accuracy, completeness, or usefulness of any information, apparatus, product, or process disclosed, or represents that its use would not infringe privately owned rights. Reference herein to any specific commercial product, process, or service by its trade name, trademark, manufacturer, or otherwise, does not necessarily constitute or imply its endorsement, recommendation, or favoring by the United States Government or any agency thereof, or the Regents of the University of California. The views and opinions of authors expressed herein do not necessarily state or reflect those of the United States Government or any agency thereof or the Regents of the University of California.

EXPERIMENTAL TEST OF THE $\Delta S = \Delta Q$ RULE IN
LEPTONIC DECAYS OF NEUTRAL K MESONS*

Bryan R. Webber, Frank T. Solmitz, Frank S. Crawford, Jr.,
and Margaret Alston-Garnjost

Lawrence Radiation Laboratory
University of California
Berkeley, California 94720

June 1970

We report the final results of a study of the time distribution of decays of neutral K mesons produced in the reaction $K^0 + p \rightarrow \bar{K}^0 + n$. We present independent results based on 81 electronic and 38 muonic decays. Combining these with 133 ambiguous events, we find for the $\Delta S = -\Delta Q$ parameter x the value $\text{Re}(x) = 0.25^{+0.07}_{-0.09}$, $\text{Im}(x) = 0.00 \pm 0.08$. This value lies about 2.5 standard deviations away from the point $x=0$, and to this extent our experiment suggests a violation of the $\Delta S = \Delta Q$ rule. In the course of an investigation of background processes, we identify and measure the rate of the radiative decay $K_S^0 \rightarrow \pi^+ \pi^- \gamma$.

I. INTRODUCTION

In 1958, Feynman and Gell-Mann¹ proposed an empirical rule for weak interactions which has become known as the " $\Delta Q = \Delta S$ " rule. They considered a weak interaction Hamiltonian with a current-current form

$$H_{\text{weak}} = J_{\mu} J_{\mu}^{\dagger} + J_{\mu}^{\dagger} J_{\mu}, \quad (1)$$

and split the current up into nonstrange hadronic, strange hadronic, and leptonic parts:

$$J_{\mu} = N_{\mu} + S_{\mu} + L_{\mu}. \quad (2)$$

The rule is concerned, then, only with the strange hadronic current S_{μ} , and states that the strangeness of this current is equal to its charge, which is +1. Thus the operators S_{μ} and S_{μ}^{\dagger} can connect only hadronic states whose strangeness and charge differ by the same amount; that is, S_{μ} (or S_{μ}^{\dagger}) induces $\Delta S = \Delta Q = +1$ (or -1) transitions.

The rule was originally proposed to account for the observation of the cascade decay

$$\Xi^- \rightarrow \Lambda \pi^-, \quad \Lambda \rightarrow n \pi^0, \quad (3)$$

instead of the direct transition

$$\Xi^- \rightarrow n \pi^-, \quad (4)$$

for if there existed a current S_{μ}^{\dagger} with $S=-Q=-1$, then the term $S_{\mu}^{\dagger} S_{\mu}$ would induce the transition (4), for example, via a Λ intermediate state:

$$\langle n \pi^- | S_{\mu}^{\dagger} | \Lambda \rangle \langle \Lambda | S_{\mu} | \Xi^- \rangle \neq 0. \quad (5)$$

Study of the hadron currents in nonleptonic processes such as (4), however, is complicated by our ignorance of strong-interaction dynamics.² This complication is greatly reduced in the leptonic decays of strange particles, in which the relevant terms of H_{weak} are $S_{\mu} L_{\mu}^{\dagger}$ and $S_{\mu}^{\dagger} L_{\mu}$, since the leptonic current is very well understood. Thus good quantitative tests of the

$\Delta S = \Delta Q$ rule did not become possible until the acquisition of large numbers of strange-particle leptonic decays. Table I shows the status of the rule in these processes, prior to our experiment.³

Table I. Tests of the $\Delta S = \Delta Q$ rule.

Process	$\Delta S/\Delta Q$	$ g'_S/g_S $	Current
$\Sigma^+ \rightarrow n \ell^+ \nu$	-1	< 0.20	V and A
$\Sigma^- \rightarrow n \ell^- \bar{\nu}$	+1		
$K^+ \rightarrow \pi^+ \pi^+ e^- \bar{\nu}$	-1	< 0.23	A
$K^+ \rightarrow \pi^+ \pi^- e^+ \nu$	+1		dominates
$K^0 \rightarrow \pi^+ \ell^- \bar{\nu}$	-1	0.21 ± 0.07	pure V
$K^0 \rightarrow \pi^- \ell^+ \nu$	+1		

In this table, ℓ represents a lepton (e or μ) and g_S and g'_S are the coupling constants of the $\Delta S = \Delta Q$ current S_μ and the $\Delta S = -\Delta Q$ current S'_μ respectively. One may separate these currents into their vector and axial vector parts; and the last column of the table shows which part contributes in each process. The $K_{\ell 3}^0$ decays provide the only test of the $\Delta S = \Delta Q$ rule for a pure vector current.

Since 1963, when the Cabibbo theory⁴ was introduced, the $\Delta S = \Delta Q$ rule has been a basic tenet of weak interaction theory. Cabibbo proposed that the hadronic weak currents are the charged members of an octet representation of the higher symmetry group SU(3). Then the strange currents transform under SU(3) like K^+ and K^- mesons, and, in particular, they have $S = Q = \pm 1$. We see from the Gell-Mann-Nishijima formula

$$Q = I_3 + \frac{1}{2} S, \quad (6)$$

where I_3 is the third component of the isospin, that a current with $S = -Q = \pm 1$, on the other hand, has $I_3 = \pm 3/2$, and cannot be a member

of an octet. Thus a violation of the $\Delta S = \Delta Q$ rule would be evidence of currents belonging to other SU(3) multiplets. In view of this, suggestions by previous experiments⁵ of a violation in the $K_{\ell 3}^0$ decays, as indicated in Table I, are of great interest. Our experiment was undertaken in order to shed more light on the validity of the rule in these decays.

We obtained \bar{K}^0 mesons by exposing the 25-inch Lawrence Radiation Laboratory hydrogen bubble chamber to a K^- beam with momenta in the range 310 to 430 MeV/c. In a total of 1.3 million pictures, we found about 18000 reactions of the type $K^- p \rightarrow \bar{K}^0 n$ followed by a visible decay of the neutral K meson. Most of these are $\pi^+ \pi^-$ decays, but we have found 252 events in which the decay is leptonic or radiative: neutral $K \rightarrow \pi^\pm e^\mp \nu$, $\pi^\pm \mu^\mp \nu$, or $\pi^+ \pi^- \gamma$. In 119 of these events the decay is definitely leptonic, and we regard the remaining 133 as completely ambiguous between the leptonic and radiative decay hypotheses. Using these 252 events, we are able to test the $\Delta S = \Delta Q$ rule with an accuracy comparable to that of any previous individual experiment.⁶ Our results may be interpreted as giving a value of $|g'_S/g_S|$ of $0.25^{+0.07}_{-0.09}$. Although we do not regard this result as conclusive evidence of a violation of the rule, it does provide support for previous indications of a violation.

Our test of the $\Delta S = \Delta Q$ rule was based on a study of the time distributions of the leptonic decays. If f is the amplitude for $K^0 \rightarrow \pi^- + e^+ + \nu$ ($\Delta S = \Delta Q$) and g is that for $\bar{K}^0 \rightarrow \pi^- + e^+ + \nu$ ($\Delta S = -\Delta Q$), for a particular final-state configuration, then the time distribution of electronic decays of an initial \bar{K}^0 state is given by⁷

$$\Gamma_e(x; q, t) = \frac{1}{4} |f|^2 [|1+x|^2 e^{-\lambda_S t} + |1-x|^2 e^{-\lambda_L t} - 2 \{ 2 \text{Im}(x) \sin \delta t + q(1-|x|^2) \cos \delta t \} e^{-\frac{1}{2}(\lambda_S + \lambda_L)t}], \quad (7)$$

where q is the charge of the electron, x is the ratio g/f , λ_S and λ_L are the K_S and K_L total

decay rates, and δ is the mass difference $m(K_S) - m(K_L)$.⁸ If the amplitude ratio x is approximately independent of the final-state configuration, we may take Eq. (7) to express the time distribution summed over all configurations, with $|f|^2$ now representing an integrated intensity, weighted by our detection efficiency for each configuration.

After further assumptions, which are discussed in full in Ref. 9, the time distribution of the muonic decays may also be shown to be of the form given in Eq. (7), with new parameters f' and x' corresponding to f and x . If there is no significant induced scalar interaction in the muonic decay process, then $x' = x$.

Clearly, the $\Delta S = \Delta Q$ rule requires $x = x' = 0$. Conservation of CP in the decay process would imply $\text{Im}(x) = \text{Im}(x') = 0$.

II. EXPERIMENTAL PROCEDURE

A. Scanning and Selection of Candidates

The 400-MeV/c K^- beam at the Bevatron, which was used for this experiment, has been fully described elsewhere.¹⁰ By movement of our target, and by use of a beryllium beam degrader, we were able to obtain data in the K^- momentum range 310 to 430 MeV/c. However, 75% of the data were taken in the range 370 to 410 MeV/c.

Typically, our bubble chamber pictures contained about six K^- and two background tracks. The background consisted of pions, muons, and some electrons. Since the background tracks had practically minimum ionization, they were easy to distinguish from the K^- tracks, which had 2.6 times minimum ionization.

The appearance of a leptonic neutral K decay in our photographs is characterized by a zero-prong and a V. The pictures were therefore scanned for V's. If both a V and a zero-prong were found, the event was measured on a Spiral Reader or Franckenstein automatic measuring machine, and we used the kinematics fitting program SIOUX to attempt four-

constraint (4C) fits to \bar{K}^0 and Λ production and two-body decay. If the confidence level for the \bar{K}^0 fit was less than 5×10^{-4} and the V was not identified as a Λ decay during scanning, fits to all three-body K-decay hypotheses were tried. If the confidence level for any of these was greater than 0.02, the event was called a three-body K^0 decay candidate and was remeasured on a Franckenstein measuring machine.

Pictures in which the scanner recorded a V but no zero-prong, and did not definitely identify the V as a Λ decay by ionization or stopping of the positive track, were carefully rescanned for zero-prongs and measured if one was found.

In about 9% of our pictures, there was a V and two or more zero-prongs, none of which was clearly associated with another event. After measuring a sample of these, we found that in 43% of them we could obtain more than one \bar{K}^0 production and three-body-decay fit, in which the same V was associated with different zero-prongs. Since the resolution of such ambiguities is likely to depend on the distance of the V from the various zero-prongs, this could give rise to a bias in the decay-time distributions. We avoided this possibility by rejecting from our set of candidates all those in pictures containing extra zero-prongs not clearly associated with other events. In this way we obtained those K^0 's which were associated with a unique production vertex, but fitted only the 1C \bar{K}^0 production and three-body-decay hypotheses.

B. Geometrical Cuts

In order to eliminate time-dependent biases from our sample of three-body decay candidates, we applied the following geometrical selection criteria. Complete discussion of these criteria and their effects may be found in Ref. 9.

We removed time-dependent biases associated with the finite size of the visible region

of the bubble chamber by placing the boundaries of the fiducial volume 8.5 cm from the top and bottom windows of the chamber, and at least 6 cm from the other limits of the visible region. The most serious bias of this kind arises from a loss of momentum resolution for short decay tracks,¹¹ and we found from Monte Carlo studies that such an effect becomes significant only when the projected length of a decay track is limited to less than 5 cm by the finite size of the chamber. We therefore required the dip angles of the decay tracks to be less than 55 deg; in conjunction with the fiducial volume, this criterion ensured that the projected lengths were not limited to less than $8.5 \cot(55 \text{ deg}) = 6$ cm.

To remove the scanning bias against events with short neutral tracks, we rejected a candidate if the decay vertex, projected onto the average plane of the camera views, lay inside a rectangular region extending 3.5 mm ahead of the production vertex, 2.5 mm behind it, and 1.75 mm to each side. These dimensions were based on a study of the same bias in a sample of 5000 decays of the type $K_S \rightarrow \pi^+ \pi^-$.

We rejected events in which the opening angle of the V was less than 2 deg or greater than 170 deg. This cut removed a large number of conversion electron pairs, and also most of those pictures in which the V was not the decay of a neutral particle, but rather the decay or small-angle scattering of an incoming charged particle.

C. Elimination of Background

Very large numbers of potential background events were eliminated by the preliminary selection criteria and geometrical cuts discussed in Secs. II A and B, for reasons that should be clear from that discussion. Nevertheless, at this stage of the analysis we had 758 leptonic decay candidates, of which less than half were expected to be true leptonic decays. Most of the other events were $K_S \rightarrow \pi^+ \pi^-$

decays which for some reason failed the 4C \bar{K}^0 production and two-body decay fit. We removed nearly all this background by means of the following three cuts. We discuss later the effects of our cuts on leptonic decays.

(a) We made 1C fits to \bar{K}^0 production and two-pion decay, in which first one and then the other pion was considered unmeasured. Clearly, an otherwise good two-body decay with one bad pion track should give a good fit when the bad track is not used. Furthermore, in such a fit the initial momentum and direction of the "unmeasured" pion are reconstructed by momentum conservation from the other tracks, and, if the bad track had a small decay or scattering kink, it should still lie close to this reconstructed direction. The appropriate criterion of "closeness" is the quantity $F = p_{\text{fit}} \beta_{\text{fit}} \Delta\theta$, where p_{fit} is the reconstructed momentum, $c\beta_{\text{fit}}$ is the corresponding velocity, and $\Delta\theta$ is the space angle between the measured and reconstructed initial directions of the track.¹² In our experiment all except 0.5 of the Coulomb scatterings, and all the decays, on the pion tracks should give values of F less than 2200 (MeV/c) deg. We therefore rejected all events giving a fit of this kind with confidence level greater than 1.5×10^{-3} and F less than 2200 (MeV/c) deg.

(b) To remove most of the radiation decays, we made a 1C fit to \bar{K}^0 production and $\pi^+ \pi^- \gamma$ decay. Unfortunately, muonic decay events have a tendency to fit this hypothesis, because of the similarity of the pion and muon masses, so we could not simply reject all events for which a fit was obtained. However, the great majority of radiative decays produce a photon of very low momentum in the center-of-mass frame, whereas the neutrino spectrum in muonic decay is expected to approach zero at low momenta. We therefore compromised by rejecting events of which this fit had a confidence level greater than 1.5×10^{-3} and a c.m. photon momentum less than 50 MeV/c. This

left a small number of radiative decays with photons of higher momentum, for which we had to correct our leptonic decay distributions. The calculation of this correction is discussed in Sec. IIIA.

(c) A significant number of two-pion decays failed the normal fit for more than one reason, giving rise to "second-order" background. The principal sources of these events were (i) $\pi^+\pi^-$ decays in which both decay pions Coulomb scattered, (ii) \bar{K}^0 's produced radiatively or after K^- scattering and decaying to $\pi^+\pi^-\gamma$ or to $\pi^+\pi^-$ followed by pion scattering, (iii) $\pi^+\pi^-\gamma$ decays followed by pion scattering, and (iv) $\pi^+\pi^-\gamma\gamma$ decays. We expect less than three events of these types to have decay photons with c.m. momenta greater than 10 MeV/c, or pion scattering with F [see (a) above] greater than 376 (MeV/c) deg. We therefore made a special fit in which we increased the errors on the tracks of the V , to take into account the possible emission of 10-MeV/c photons in the decay and a subsequent scattering with $F = 376$ (MeV/c) deg. This 3C fit was to the two-pion decay of a neutral K coming from the direction of the zero-prong; we did not use the momentum or direction of the beam track, so second-order background events with a bad beam track or radiative production vertex should also give a good fit. We rejected all events giving a confidence level greater than 0.1 for this special fit. In view of the large kinematic overlap between this cut and the preceding two, we estimate that less than 1.5 second-order background events should remain after the application of all three cuts.

Having made the above cuts, we were left with 452 candidates, which we examined on a scanning table. We could then make a number of cuts which depended in part on the results of this examination.

(d) One-constraint fits were made to the two-body decay of a Λ or neutral K of unknown origin.

An event was rejected if it gave a confidence level greater than 5×10^{-4} and the appearance of the V was consistent with the corresponding interpretation. This cut eliminated two-body decays in which the beam track measurement was bad, the production process was radiative, or the neutral particle scattered or interacted in flight. It also eliminated two-body "wall V 's," that is, decays of neutral particles produced outside the visible region which were mistakenly associated with a zero-prong in the picture.

(e) The tracks of the V were interpreted as electrons, if this was consistent with their ionization, and the invariant mass of the pair was calculated. If this was less than 140 MeV, the event was rejected. This cut removed γ -ray conversion pairs, and also decays of the forms $K_S \rightarrow \pi^0\pi^0$, $\pi^0 \rightarrow e^+e^-\gamma$ and $\Lambda \rightarrow n\pi^0$, $\pi^0 \rightarrow e^+e^-\gamma$.

(f) In some events, it could not be definitely established by inspection that both particles in the V were moving out from the vertex. This raised the possibility that the V was the decay of an incoming muon, or the decay or elastic scattering of an incoming charged pion. When a V appeared to be consistent with one of these hypotheses, we calculated the missing mass at the vertex with the appropriate track reversed, and, for the π and μ decays, rejected the event if the square of this lay within four standard deviations of a correct value [0 for the pion decay and the range 0 to (105 MeV)² for the muon decay]. For the pion scattering hypothesis, we also required the recoiling proton to be invisible [missing momentum squared within four standard deviations of the range 0 to (80 MeV/c)²] before rejecting an event.

We believe that cuts (a) through (f) cover all significant sources of background in our experiment.¹³ The decay mode neutral $K \rightarrow \pi^+\pi^-\pi^0$ is kinematically quite distinct from the leptonic decays and gives rise to no back-

ground. In a sample of 1.6×10^5 pictures, we made a search for three-body wall V's, which might give spurious leptonic fits with unassociated zero-prongs in the same picture. In this sample, there were 29 wall V's inside our decay fiducial volume. For each wall V, we simulated an unassociated zero-prong by measuring a beam track associated with a real event in the same picture. None of the combinations of zero-prong plus wall V survived our selection criteria for leptonic decays.

We have studied the effects of cuts similar to those discussed above on 3616 simulated leptonic decays, generated by the Lawrence Radiation Laboratory program PHONY.¹⁴ This program reduces Monte Carlo events to sets of coordinate points, simulating the output from a measuring machine. The K^- and \bar{K}^0 distributions of the Monte Carlo events were deduced from the real $K_S^0 \rightarrow \pi^+ \pi^-$ events at the beam momentum setting at which we took most of our data. For the decay distributions, we assumed $\Delta S = \Delta Q$ and used the standard current-current interaction matrix element, setting the form factor ratio ξ equal to zero for the muonic decays. We found that about 50% of the simulated events were rejected. Those remaining showed no biases in their decay-time distributions, and gave good agreement with the $\Delta S = \Delta Q$ rule when analyzed by the methods discussed in Sec. III B.

D. Identification of Leptons

We have been able to identify the lepton in 119 of the 252 events remaining after the selection procedures described in the previous section. Of the identified leptons, 32 were e^+ , 49 e^- , 14 μ^+ , and 24 μ^- .

We identified 78 of the 81 electrons and 25 of the 38 muons by comparison of track densities during scanning-table inspection of the events. A computer program was used to predict the projected relative ionization for each mass hypothesis for each track, at the

beginning and end of the measured track segment in each of the three camera views. If these predictions were judged to be consistent with the observed event for only one decay hypothesis, the event was considered to be identified.

If a lepton could not be positively identified by inspection, we considered the event to be completely ambiguous between the leptonic and $\pi\pi\gamma$ decay hypotheses. We made no use of kinematic confidence levels in identifying events, because we found evidence from simulated events that the resolution of kinematically similar hypotheses, such as $\pi^+ \mu^- \nu$, $\pi^- \mu^+ \nu$, and $\pi^+ \pi^- \gamma$, depends on the distance between the zero-prong and the V, and hence on the time of flight of the neutral K. We therefore chose to make no resolutions on the basis of kinematics, rather than to introduce a time-dependent resolution function based entirely on a Monte Carlo simulation.

It is clear that leptonic tracks of small projected length cannot be identified, because their ionization cannot be observed with sufficient precision. We believe, however, that the minimum projected length of 6 cm (4 cm on the scanning table) provided by our fiducial-volume and dip-angle cuts is sufficient to eliminate any significant bias of this kind, and, indeed, the results of our analysis are not significantly affected if we make these cuts more restrictive.

In 3 electronic and 13 muonic decays, identification was made with the help of information other than track density. Sources of information were δ -ray momenta for electrons,¹⁵ and decays and comparison with curvature templates for muons. The probability of obtaining information of these kinds does depend on the position of the decay vertex in the bubble chamber. However, in view of the small number of events identified in these ways, we do not believe that this effect gives rise to a significant bias in the time distributions. Indeed, if we

make no use of information other than track density, and treat these 16 events as unidentified, the results of our analysis are not significantly affected.

As a final check that our lepton identification procedures do not introduce biases, we have performed an analysis in which we treat all 252 of our events as unidentified. The results are consistent with those of the full analysis discussed in Sec. III B.

An important feature of our selection criteria and methods of lepton identification is that they are all charge symmetric. The numbers of identified positive and negative leptonic decays therefore provide information, as well as the shapes of the decay-time distributions. Furthermore, the predicted time distribution of the ambiguous events is proportional to the sum of the positive and negative leptonic decay-time distributions, corrected for the expected $\pi^+\pi^-\gamma$ contamination, which we discuss in Sec. III A. In Sec. III B, we describe how these facts are used in the maximum-likelihood analysis of our data.

III. ANALYSIS AND RESULTS

A. Correction for Remaining Background

As discussed in Sec. II C, the principal background remaining after our cuts consists of radiative two-pion decays with c.m. photon momenta greater than 50 MeV/c. These events cannot be satisfactorily removed from our sample of ambiguous events because they are kinematically very similar to muonic decays, so we have had to apply a correction based on theoretical predictions of the number and distributions of radiative decays. We estimate that other sources of background contribute less than two events with the K_S lifetime and about 0.5 with the K_L lifetime. We have not corrected for these events.

To compute the correction for radiative two-pion decay, we assume that this process occurs only through inner bremsstrahlung of

the mode $K_S \rightarrow \pi^+\pi^-$. This hypothesis is supported by earlier experimental data¹⁶ and by our own, which we discuss at the end of this section. The inner bremsstrahlung spectrum has been calculated,¹⁷ and leads to the prediction

$$\Gamma(K_S \rightarrow \pi^+\pi^-\gamma; k) \approx 50 \text{ MeV/c} \\ = (2.56 \times 10^3) \Gamma(K_S \rightarrow \pi^+\pi^-), \quad (8)$$

where k is the photon momentum in the overall c.m. system.

Since the $\pi^+\pi^-\gamma$ decays should have the same time distribution as the $\pi^+\pi^-$ decays, the predicted number of $\pi^+\pi^-\gamma$ decays is given by

$$n_\gamma = (2.56 \times 10^3) \frac{\epsilon_\gamma}{\epsilon_{2\pi}} n_{2\pi}. \quad (9)$$

Here $\epsilon_{2\pi}$ is the efficiency of any set of cuts that removes all background and scanning biases from our sample of $\pi^+\pi^-$ decays, and $n_{2\pi}$ is the observed number of such decays after these cuts; ϵ_γ is the efficiency of our selection criteria for leptonic decays when applied to $\pi^+\pi^-\gamma$ decays, that is, the probability that a $\pi^+\pi^-\gamma$ decay will satisfy all these criteria and be included in our sample of 252 events.

To evaluate $n_{2\pi}$ and $\epsilon_{2\pi}$, we subjected real and simulated $\pi^+\pi^-$ decays to a set of cuts designed to eliminate all background and scanning biases. For uniformity, we rejected events having a decay-track dip angle greater than 55 deg or less than -55 deg, as we did with the leptonic decays. We found $n_{2\pi} = 12\,833$ after these cuts, and $\epsilon_{2\pi} = 66\%$. This low efficiency was due almost entirely to the dip-angle cut, which removed 31% of the simulated $\pi^+\pi^-$ decays.

We applied selection criteria similar to those described in Sec. II to simulated $\pi^+\pi^-\gamma$ decays, and found $\epsilon_\gamma = 0.65$. This is considerably higher than the estimated efficiency for true leptonic decays (about 0.50), since the high photon momentum makes $\pi^+\pi^-\gamma$ decays with $k > 50$ MeV/c less likely to be rejected as possible $\pi^+\pi^-$ background.

Since some of our selection criteria involve scanning-table examination of the event, we were unable to estimate ϵ_γ with great precision from simulated events, which could not, of course, be so examined. However, after varying our assumptions about the importance of scanning information within reasonable limits, we are confident that our estimate of ϵ_γ is accurate within 5%, which is more than adequate for calculating the required correction to our data.

The predicted number of background $\pi^+\pi^-\gamma$ decays in our sample of 133 ambiguous events is now given by Eq. (9):

$$n_\gamma = 31.4 \text{ events.} \quad (10)$$

In Sec. III B we discuss how this number is used to make a correction to the likelihood function in the maximum-likelihood analysis.

We expect a small but significant number of kinematically unambiguous $\pi^+\pi^-\gamma$ decays in our experiment, since we find, from further analysis of simulated events, a probability $\epsilon_{\gamma u} = 0.157$ that a $\pi^+\pi^-\gamma$ decay will satisfy all our selection criteria, have only three-body decay fits, and have a confidence level for the $\pi^+\pi^-\gamma$ fit that is greater than 2% and more than 50 times that of the second-best fit. This leads to a predicted number $n_{\gamma u}$ of unambiguous $\pi^+\pi^-\gamma$ decays, where

$$n_{\gamma u} = (2.56 \times 10^{-3}) \frac{\epsilon_{\gamma u}}{\epsilon_{2\pi}} n_{2\pi} = 7.6 \text{ events.} \quad (11)$$

The background of leptonic decays in this sample should be less than 0.3 event. In fact, we find 10 events which are unambiguous, according to the above criteria. Both their c.m. photon momentum and decay-time distributions are in good agreement with those of simulated $K_S \rightarrow \pi^+\pi^-\gamma$ decays, generated with an inner bremsstrahlung distribution and subjected to the same cuts. These 10 events therefore provide additional experimental support for our hypothesis that $\pi^+\pi^-\gamma$ decay occurs only through

this process. They give a value for the decay rate for $k > 50 \text{ MeV}/c$,

$$\Gamma(K_S \rightarrow \pi^+\pi^-\gamma; k > 50 \text{ MeV}/c) = (3.3 \pm 1.2) \times 10^{-3} \Gamma(K_S \rightarrow \pi^+\pi^-), \quad (12)$$

which is in agreement with the prediction given in Eq. (8). The error includes an estimated 20% uncertainty in $\epsilon_{\gamma u}$.

B. Maximum-Likelihood Analysis

The histograms in Figs. 1, 2, and 3 show the time distributions of the positive leptonic, negative leptonic, and ambiguous decays in the interval from 0 to 10^{-9} sec. There were 12 additional decays at times greater than 10^{-9} sec. We have made a maximum-likelihood analysis of the electronic, muonic, and ambiguous decay-time distributions in terms of the parameters x and x' defined in Sec. I. In this analysis we have used events at all decay times, but our results are in fact completely insensitive to the distribution of the 12 events not shown in the histograms. The solid and broken curves in Figs. 1, 2, and 3 are explained in Sec. III C.

Consider first the identified electronic decays. The likelihood of a given value of x , $\mathcal{L}_e(x)$ is simply the probability that, if x truly had this value, the distributions of these events would be as we observed them. Suppose that in the i th event we looked at an interval of proper time from t_{\min}^i to t_{\max}^i , and observed a decay with electron charge q^i at time t^i . For every event in our sample, the uncertainty in the decay time is less than 12%, and we neglect it. First, given that the electron had charge q^i , the differential probability that the decay should occur at time t^i is

$$\Gamma_e(x; q^i, t^i) / \int_{t_{\min}^i}^{t_{\max}^i} \Gamma_e(x; q^i, t) dt,$$

which is normalized to the interval t_{\min}^i to t_{\max}^i (with constant detection efficiency) since

the decay was actually observed in this interval. Furthermore, the probability that the electron should have charge q^i , rather than $-q^i$, in a decay in this interval, is

$$\int_{t_{\min}^i}^{t_{\max}^i} \Gamma_e(x; q^i, t) dt / \int_{t_{\min}^i}^{t_{\max}^i} [\Gamma_e(x; +1, t) + \Gamma_e(x; -1, t)] dt,$$

since our selection and identification procedures are charge-symmetric. The likelihood function is then the product of these two factors for every identified electronic decay:

$$\mathcal{L}_e(x) = \prod_{i=1}^{81} \frac{\Gamma_e(x; q^i, t^i)}{\int_{t_{\min}^i}^{t_{\max}^i} [\Gamma_e(x; +1, t) + \Gamma_e(x; -1, t)] dt} \quad (13)$$

A contour plot of this function in the x complex plane is shown in Fig. 4. We have drawn contours at likelihood values $\exp(-\frac{1}{2}n^2)$ relative to the likelihood peak, for $n = 1, 2, 3, 4$, and 5 . The location of the peak is shown by the solid circle. If the errors in $\text{Re}(x)$ and $\text{Im}(x)$ were Gaussian and uncorrelated, the contours shown would be right ellipses of constant separation, representing numbers of standard deviations from the peak. We see that this is approximately the case for small n , so our result for the 81 identified electronic decays may be written

$$\text{Re}(x) = 0.30_{-0.12}^{+0.10}, \quad \text{Im}(x) = 0.07_{-0.08}^{+0.10}, \quad (14)$$

where the errors in $\text{Re}(x)$ and $\text{Im}(x)$ are essentially uncorrelated and represent one-standard-deviation limits.

We treated the identified muonic decays in the same way, defining the likelihood function for x' as

$$\mathcal{L}_\mu(x') = \prod_{i=1}^{38} \frac{\Gamma_\mu(x'; q^i, t^i)}{\int_{t_{\min}^i}^{t_{\max}^i} [\Gamma_\mu(x'; +1, t) + \Gamma_\mu(x'; -1, t)] dt} \quad (15)$$

where $\Gamma_\mu(x'; q, t)$ is the time-dependent rate of decay for muon charge q , corresponding to Eq. (7). A contour plot of this likelihood function is shown in Fig. 5, and gives as our result for the 38 identified muonic decays

$$\text{Re}(x') = 0.19_{-0.18}^{+0.13}, \quad \text{Im}(x') = -0.12_{-0.17}^{+0.20}. \quad (16)$$

As in our result (14) for the electronic decays, the errors in (16) are essentially uncorrelated and are one-standard-deviation limits.

The results (14) and (16) are clearly consistent with the hypothesis $x = x'$, which corresponds to a negligible contribution of the induced scalar interaction in both the electronic and the muonic decay modes. If we make this hypothesis, then both (14) and (16) may be regarded as measurements of the parameter x , and we may combine them to obtain the likelihood contours shown in Fig. 6, which give

$$\text{Re}(x) = 0.23 \pm 0.09, \quad \text{Im}(x) = 0.04 \pm 0.08, \quad (17)$$

from the 119 identified leptonic decays.

The hypothesis that x and x' are equal also allows us to use the ambiguous events to measure their common value. However, our sample of 133 ambiguous events is expected to contain $31.4 \pi^+ \pi^- \gamma$ decays, discussed in Sec. III A, so we must apply a correction for these background events in the likelihood function. The corrected function has the form¹⁸

$$\mathcal{L}_0(x) = \prod_{i=1}^{133} \frac{P(x; +1, t^i) + P(x; -1, t^i) + f_c(x) \exp(-\lambda_S t^i)}{\int_{t_{\min}^i}^{t_{\max}^i} [P(x; +1, t) + P(x; -1, t) + f_c(x) \exp(-\lambda_S t)] dt} \quad (18)$$

where $P(x; q, t)$ is the unnormalized distribution $P(x; q, t) = 4\Gamma_e(x; q, t) / |f|^2 = |1+x|^2 e^{-\lambda_S t} + |1-x|^2 e^{-\lambda_L t} - 2[2\text{Im}(x)\sin\delta t + q(1-|x|^2)\cos\delta t] e^{-\frac{1}{2}(\lambda_S + \lambda_L)t}$, and $f_c(x)$ is the correction function

$$f_c(x) = \frac{31.4}{133-31.4} \frac{\int_0^\infty [P(x; +1, t) + P(x; -1, t)] \epsilon(t) dt}{\int_0^\infty \exp(-\lambda_S t) \epsilon(t) dt} \equiv 0.309 Q(x), \quad (20)$$

where $\epsilon(t)$ is the geometrical efficiency function for our experiment, which is shown in Fig. 7. The correction depends on x because we wish to keep the fraction of $\pi^+\pi^-\gamma$ decays constant at 31.4/133, while allowing x to vary. Performing the integrations in Eq. (20), we find

$$Q(x) = 2|1+x|^2 + 24.6|1-x|^2 + 10.0 \operatorname{Im}(x). \quad (24)$$

Using the corresponding correction in the likelihood function (18), we obtain from the 133 ambiguous events the result

$$\operatorname{Re}(x) = 0.32 \pm 0.12, \quad \operatorname{Im}(x) = -0.27_{-0.20}^{+0.17}. \quad (22)$$

A contour plot of the likelihood is shown in Fig. 8. Combining this likelihood with those for the identified events, we obtain the plot in Fig. 9. The corresponding value of x , determined from all 252 events, is

$$\operatorname{Re}(x) = 0.25_{-0.09}^{+0.07}, \quad \operatorname{Im}(x) = 0.00 \pm 0.08. \quad (23)$$

We stress again that this result, unlike (14) and (16), is meaningful only if $x = x'$, that is, only if the contributions made by induced scalar and pseudoscalar interactions are negligible in both the electronic and the muonic decays. This is not well established, but the results for our identified events are consistent with this hypothesis.

C. Consistency Tests

A maximum-likelihood analysis gives the relative likelihood of various values of the parameters being measured, but does not indicate whether any of these values gives a good fit to the data. If the parameterization of the time distributions in terms of x is entirely inappropriate, then even our most likely value of x , given by Eq. (23), gives a bad fit to these distributions. We investigated this possibility by making the following three tests of the consistency of our data with the parameterization used.

1. χ^2 test of the time distributions

The predicted time distributions of the

positive leptonic, negative leptonic, and unidentified decays are, respectively,

$$\begin{aligned} \frac{dn^+}{dt}(x; t) &= N_1 P(x; +1, t) \epsilon(t), \\ \frac{dn^-}{dt}(x; t) &= N_1 P(x; -1, t) \epsilon(t), \\ \frac{dn^0}{dt}(x; t) &= N_u [P(x; +1, t) + P(x; -1, t) \\ &\quad + f_c(x) \exp(-\lambda_S t)] \epsilon(t), \end{aligned} \quad (24)$$

where $\epsilon(t)$ is the geometrical efficiency, shown in Fig. 7, and N_1 and N_u are normalization constants. We normalize to the observed numbers of identified and unidentified events; since the selection and identification procedures were charge-symmetric, we use the same normalization constant N_1 for the positive and negative leptonic distributions. The predictions for $x = 0$ ($\Delta S = \Delta Q$) and x given by Eq. (23) are shown in Figs. 1, 2, and 3 by the solid and broken curves, respectively.

For the ten decay-time bins shown in the three distributions, the overall values of χ^2 were 27.0 for the $\Delta S = \Delta Q$ prediction and 26.1 for our result (23). The expectation values of χ^2 were, respectively, 28 (30 bins and 2 normalizations) and 26 (two independent free parameters). We conclude that, over the time interval from 0 to 10^{-9} sec, both curves give satisfactory fits to the data. We did not use decay times greater than 10^{-9} sec in the χ^2 test, since these bins would contain too few events to give meaningful χ^2 contributions. Even in the interval used, some of the bins contain only one or two events, and the χ^2 provides only a rough test of consistency which is rather insensitive to the parameter x . Of course, these criticisms do not apply to a maximum-likelihood analysis, and for this we used events at all decay times. However, we found that our results were in fact insensitive to the distribution of events beyond 4×10^{-10} sec. For the interval from 0 to 4×10^{-10} sec, in which the statistics are best and the χ^2

should be most sensitive to x , we found χ^2 contributions of 10.8 and 5.3 for $\Delta S = \Delta Q$ and our result (23), respectively, reflecting the greater likelihood of the latter value.

We conclude that the χ^2 test shows a parameterization in terms of x to be appropriate, and is consistent with our likelihood analysis.

2. Measurement of the K_L leptonic decay rate

Although our analysis of the decay-time distributions was independent of the normalization constants N_i and N_u , it was necessary to check the values of these quantities for unexplained losses of events, which might be time-dependent and thus give rise to incorrect results. The only previously well-measured quantity with which we may compare our normalization is the leptonic decay rate of the K_L , $\Gamma_L(\ell)$. Noting that

$$P(x; \pm 1, t) = |1-x|^2 \text{ when } \lambda_S^{-1} \ll t \ll \lambda_L^{-1}, \quad (25)$$

we have an observed leptonic decay rate of

$$2(N_i + N_u) |1-x|^2 \epsilon(t) = \frac{1}{2} N \epsilon_\ell \epsilon(t) \Gamma_L(\ell) \quad (26)$$

$$\text{for } \lambda_S^{-1} \ll t \ll \lambda_L^{-1},$$

where N is the number of \bar{K}^0 's produced in our fiducial volume and ϵ_ℓ is the time-independent part of our detection efficiency for leptonic decays. The total number of leptonic decays seen is

$$\begin{aligned} n_\ell &= (N_i + N_u) \int_0^\infty [P(x; +1, t) \\ &+ P(x; -1, t)] \epsilon(t) dt, \\ &= \frac{1}{2} N \epsilon_\ell \Gamma_L(\ell) \frac{1}{2|1-x|^2} \int_0^\infty [P(x; +1, t) \\ &+ P(x; -1, t)] \epsilon(t) dt. \end{aligned} \quad (27)$$

We calculate N , the number of \bar{K}^0 's, from the observed number $n_{2\pi}$ of $K_S \rightarrow \pi^+ \pi^-$ decays; we have

$$n_{2\pi} = \frac{1}{2} N \epsilon_{2\pi} \Gamma(K_S \rightarrow \pi^+ \pi^-) \int_0^\infty \exp(-\lambda_S t) \epsilon(t) dt, \quad (28)$$

where $\epsilon_{2\pi}$ is the time-independent part of the detection efficiency for $\pi^+ \pi^-$ decays. This gives

$$\Gamma_L(\ell) = 2 \frac{\epsilon_{2\pi}}{\epsilon_\ell} \frac{n_\ell}{n_{2\pi}} |1-x|^2 [Q(x)]^{-1} \Gamma(K_S \rightarrow \pi^+ \pi^-), \quad (29)$$

where $Q(x)$ is the ratio of integrals given in Eq. (24).

In order to evaluate accurately the efficiency ϵ_ℓ by means of the Monte Carlo program PHONY, we had to modify some of our cuts to remove their dependence on qualitative scanning information. For example, in the set of cuts for the test of $\Delta S = \Delta Q$, in which it was not necessary to know ϵ_ℓ , we rejected an event in which the V fitted an incoming muon or charged pion decay only when its appearance (ionization, energy-loss, δ rays, etc.) was consistent with this interpretation. In our cuts for the calculation of the K_L leptonic decay rate, since PHONY could not be made to simulate such complicated criteria, we simply rejected all events satisfying the kinematic criteria for this cut, independent of appearance. Because of these and other similar changes, only 205 of our 252 events were used for the calculation of $\Gamma_L(\ell)$, and the efficiency ϵ_ℓ was found from simulated events to be 41%. The predicted contamination of $\pi^+ \pi^- \gamma$ decays was 27.3 events, so that $n_\ell = 177.7$ events.

The determination of $n_{2\pi}$ and $\epsilon_{2\pi}$ was discussed in Sec. III A.

It may be seen from Eq. (29) that our measurement of $\Gamma_L(\ell)$ depends on the value assumed for x . This is essentially because the total number of leptonic decays, n_ℓ , enters into the right-hand side of Eq. (29), and the fraction of these that is due to K_L decay depends on the value of x . For $x = 0$, we find $\Gamma_L(\ell) = (13.1 \pm 1.3) \times 10^6 \text{ sec}^{-1}$ and for $x = 0.25$, $\Gamma_L(\ell) = (11.5 \pm 1.4) \times 10^6 \text{ sec}^{-1}$. These values may be compared with the current world average,¹⁹ $\Gamma_L(\ell) = (12.24 \pm 0.46) \times 10^6 \text{ sec}^{-1}$. Clearly, this

test shows no sign of unexplained loss of events in our experiment. Like the χ^2 test, this test is rather insensitive to x , and gives consistent results for both $x = 0$ and the value found in the maximum-likelihood analysis.

3. Measurement of the K_S - K_L mass difference

To make a more detailed check of the time distributions than is provided by the χ^2 test and the measurement of $\Gamma_L(\ell)$, we made a maximum-likelihood determination of the mass difference δ . We used the likelihood function for all 252 events (assuming $x = x'$, as discussed in Sec. III B), allowing δ to vary first instead of, and then in addition to, x . For fixed, real values of x , this function is insensitive to the sign of δ , since the terms involving $\sin \delta t$ in the time distributions vanish when $\text{Im}(x) = 0$.

For x fixed at the value zero, as predicted by the $\Delta S = \Delta Q$ rule, we find $|\delta| = (0.47^{+0.12}_{-0.16}) \times 10^{10} \text{ sec}^{-1}$. For $x = 0.25$, we obtain $|\delta| = (0.56^{+0.09}_{-0.08}) \times 10^{10} \text{ sec}^{-1}$. These values are to be compared with the current world average value¹⁹ of $\delta = (-0.544 \pm 0.017) \times 10^{10} \text{ sec}^{-1}$. In both cases, the agreement is very good.

As a final check, we have allowed both x and δ to vary, and have made a simultaneous maximum-likelihood fit to the three quantities $\text{Re}(x)$, $\text{Im}(x)$, and δ . Here the signs of $\text{Im}(x)$ and δ are not determined, but they are coupled, since the likelihood function is invariant under a change of the signs of $\text{Im}(x)$ and δ together. Choosing the well-established negative sign for δ , we find

$$\text{Re}(x) = 0.25^{+0.08}_{-0.10}, \quad \text{Im}(x) = -0.01^{+0.17}_{-0.11}, \quad (30)$$

$$\delta = (-0.56^{+0.15}_{-0.10}) \times 10^{10} \text{ sec}^{-1}.$$

It may be seen that the value of x is essentially unchanged by this procedure, and the agreement of δ with the established value remains excellent. The small increases in the errors in x , compared with those in Eq. (23),

reflect the insensitivity of our result (23) to the value used for δ . More precisely, a change in $|\delta|$ of three "world average standard deviations, $^{19} \Delta |\delta| = \pm 0.05 \times 10^{10} \text{ sec}^{-1}$, produces a change in our most likely value of x of

$$\Delta x = \pm 0.007 \mp 0.037 i. \quad (34)$$

IV. DISCUSSION

Our result (23) is not in good agreement with the prediction of the $\Delta S = \Delta Q$ rule. The likelihood of $x = 0$, relative to the likelihood maximum, is $e^{-3.2} = 0.04$. Alternatively, we may say that the most likely value of x lies about $(2 \times 3.2)^{\frac{1}{2}} = 2.5$ standard deviations away from zero. While we do not regard a 2.5-standard-deviation effect as statistically conclusive, it does suggest a violation of the $\Delta S = \Delta Q$ rule.

The value we obtain for $\text{Im}(x)$ is consistent with zero; thus we find no evidence for a CP-nonconserving contribution to x .

It may be seen from the curves in Figs. 1, 2, and 3 that our positive result for $\text{Re}(x)$ is due mainly to an excess of about 14 negative leptons in the first $3 \times 10^{-10} \text{ sec}$, and partly to an excess of about nine unidentified events in the first 10^{-10} sec , as would result if we had not eliminated all $K_S \rightarrow \pi^+ \pi^-$ background. Accordingly we have tried increasing the severity of the cuts (a) to (f) in Sec. II C, both one at a time and in various combinations, so as to remove each time about 25 additional events from our sample. These removal have no significant effect on our results, and we are convinced that we have negligible $K_S \rightarrow \pi^+ \pi^-$ background. Furthermore, the likelihood plots in Figs. 4 and 9 show that our measurement of x is dominated by the identified electronic decays; the muonic and unidentified events add relatively little information, owing to poor statistics in one case and insensitivity to x in the other. Thus our result (23) is principally based on the set of events that is

least likely to be subject to $K_S \rightarrow \pi^+ \pi^-$ background contamination.

Figure 10 shows our result for x , together with an average of the results of earlier experiments.²⁰ The agreement is only fair: the value of χ^2 is 4.7 for two degrees of freedom, giving a confidence level of about 0.1 for consistency of the two values. Nevertheless, the results are in good enough agreement to suggest strongly that x is not zero.

In Fig. 10 we also show the results of two recent measurements of x ,^{21,22} together with the result of an experiment²³ in which the quantity

$$R = \frac{1 - |x|^2}{|1 - x|^2} \quad (32)$$

was determined by analysis of the time-dependent charge asymmetry in electronic neutral K decays. In that experiment, the measured value of R was

$$R = 0.96 \pm 0.05. \quad (33)$$

Curves of constant R are circles in the complex x plane, and the result (33) corresponds to a value of x lying somewhere in the shaded region in Fig. 10. All values of x in this region are in poor agreement with our result, which corresponds to

$$R = 1.67^{+0.27}_{-0.29}. \quad (34)$$

Values of x consistent both with earlier experiments and with result (33) are predominantly imaginary, in conflict with our measurement of $\text{Im}(x)$.

V. ACKNOWLEDGMENTS

It is a pleasure to acknowledge the interest and support of Luis W. Alvarez. We thank the 25-inch bubble chamber crew, the Bevatron crew, and our scanners and measurers for their excellent work. One of us (B.R.W.) also wishes to acknowledge the support of a N. A. T. O. Research Studentship during a part of this work.

FOOTNOTE AND REFERENCES

*Work done under auspices of the U. S. Atomic Energy Commission.

1. R. P. Feynman and M. Gell-Mann, *Phys. Rev.* **109**, 193 (1958).
2. Thus the small $\Delta S = -\Delta Q$ effect suggested by our experiment cannot at present be shown to be in conflict with the limit (0.1%) on the branching ratio for the process (4).
3. The averages of results prior to our experiment were made by A. H. Rosenfeld, N. Barash-Schmidt, A. Barbaro-Galtieri, L. R. Price, P. Söding, C. G. Wohl, M. Roos, and W. J. Willis, *Rev. Mod. Phys.* **40**, 77 (1968).
4. N. Cabibbo, *Phys. Rev. Letters* **10**, 531 (1963).
5. R. P. Ely, W. M. Powell, H. White, M. Baldo-Ceolin, E. Calimani, S. Ciampolillo, O. Fabbri, F. Farini, C. Filippi, H. Huzita, G. Miari, U. Camerini, W. F. Fry, and S. Natali, *Phys. Rev. Letters* **8**, 132 (1962); G. Alexander, S. P. Almeida, and F. S. Crawford, Jr., *ibid.* **9**, 69 (1962); B. Aubert, L. Behr, F. L. Canavan, L. M. Chounet, J. P. Lowys, P. Mittner, and C. Pascaud, *Phys. Letters* **17**, 59 (1965); M. Baldo-Ceolin, E. Calimani, S. Ciampolillo, C. Filippi-Filosofo, H. Huzita, F. Mattioli, and G. Miari, *Nuovo Cimento* **38**, 684 (1965); P. Franzini, L. Kirsch, P. Schmidt, J. Steinberger, and J. Plano, *Phys. Rev.* **140**, B127 (1965); L. Feldman, S. Frankel, V. L. Highland, T. Sloan, O. B. Van Dyck, W. D. Wales, R. Winston, and D. M. Wolfe, *Phys. Rev.* **155**, 1611 (1967); D. G. Hill, D. Luers, D. K. Robinson, M. Sakitt, O. Skjeggstad, J. Canter, Y. Cho, A. Dralle, A. Engler, H. E. Fisk, R. W. Kraemer, and C. M. Meltzer, *Phys. Rev. Letters* **19**, 668 (1967).
6. Preliminary results of our experiment, based on 242 events, were published by Bryan R. Webber, Frank T. Solmitz, Frank S. Crawford, Jr., and Margaret Alston-Garnjost, *Phys. Rev. Letters* **21**, 498 (1968); **21**, 715 (1968).

7. A complete review of the phenomenology of neutral K leptonic decays is given by T. D. Lee and C. S. Wu, *Ann. Rev. Nucl. Sci.* **16**, 511 (1966).
8. We use the values $\lambda_S^{-1} = 0.862 \times 10^{-10}$ sec, $\lambda_L^{-1} = 5.38 \times 10^{-8}$ sec, and $\delta = -0.544 \times 10^{10}$ sec⁻¹, from the compilation by the Particle Data Group, *Rev. Mod. Phys.* **41**, 109 (1969).
9. B. R. Webber (Ph.D. thesis), Lawrence Radiation Laboratory Report UCRL-19226, 1969 (unpublished).
10. Roger O. Bangertter, K-65 Beam Optics, Lawrence Radiation Laboratory Alvarez Group Physics Note 574, Oct. 1965 (unpublished).
11. We thank Dr. A. Engler (Carnegie-Mellon University, Pittsburgh, Pennsylvania) for calling our attention to this effect in a private communication, 1969.
12. This criterion was first used by Robert L. Golden, Leptonic Decays of Neutral K Mesons (Ph.D. thesis), Lawrence Radiation Laboratory Report UCRL-16771, March 1966 (unpublished).
13. Rare decay modes of the Λ do not give rise to background, because the decay proton track is easily identified by range or ionization. We neglect the possibility of processes such as neutral $K \rightarrow \mu^+ \mu^-$, which would require the existence of neutral currents.
14. E. R. Burns, Jr. (Lawrence Radiation Laboratory), and Y. Oren and D. Drijard, private communication, 1967.
15. Frank S. Crawford, Jr., Use of Delta Rays to Determine Particle Velocities, Lawrence Radiation Laboratory Internal Report UCID-241, Nov. 1957 (unpublished).
16. E. Bellotti, A. Pullia, M. Baldo-Ceolin, E. Calimani, S. Ciampolillo, H. Huzita, F. Mattioli, and A. Sconza, *Nuovo Cimento* **45A**, 737 (1966).
17. This spectrum was first calculated by M. Bég, R. Friedberg, and J. Schultz, as quoted by Franzini et al. (Ref. 5).
18. For the ambiguous events, we choose the values of t^i , t_{\min}^i , and t_{\max}^i appropriate to the best three-body decay fit. Since the best fit may occasionally be to an incorrect decay hypothesis, the expected errors in these quantities are larger than those for identified events. However, we find no evidence from our Monte Carlo simulation that this effect gives rise to biases in the time distribution of the ambiguous events.
19. All the world average values quoted are taken from the Particle Data Group compilation (Ref. 8).
20. The results used in making the average of earlier determinations of x were from experiments by Aubert et al., Baldo-Ceolin et al., Franzini et al., Feldman et al., and Hill et al. (all Ref. 5).
21. F. James and H. Briand, *Nucl. Phys.* **B8**, 365 (1968).
22. L. S. Littenberg, J. H. Field, O. Piccioni, W. A. W. Mehlhop, S. S. Murty, P. H. Bowles, and T. H. Burnett, *Phys. Rev. Letters* **22**, 654 (1969).
23. S. Bennett, D. Nygren, H. Saal, J. Steinberger, and J. Sunderland, *Phys. Letters* **29B**, 317 (1969).

FIGURE CAPTIONS

Fig. 1. Time distribution of the 46 positive leptonic decays. The solid and broken curves show the predictions for $x = 0$ and $x = 0.25$, and their integrals over the first time bin are 0.92 and 0.90, respectively.

Fig. 2. Time distribution of the 73 negative leptonic decays. The solid and broken curves show the predictions for $x = 0$ and $x = 0.25$, and their integrals over the first time bin are 15.0 and 21.6, respectively.

Fig. 3. Time distribution of the 133 unidentified events. The solid and broken curves show the predictions for $x = 0$ and $x = 0.25$, and their integrals over the first time bin are 34.4 and 39.5, respectively.

Fig. 4. Likelihood contours for the 81 identified electronic decays.

Fig. 5. Likelihood contours for the 38 identified muonic decays.

Fig. 6. Likelihood contours for the 119 identified leptonic decays. This likelihood function is the product of those in Figs. 4 and 5.

Fig. 7. Geometrical efficiency function.

Fig. 8. Likelihood contours for the 133 unidentified events.

Fig. 9. Likelihood contours for all 252 events. This likelihood function is the product of those in Figs. 6 and 8.

Fig. 10. Experimental results for the value of x .

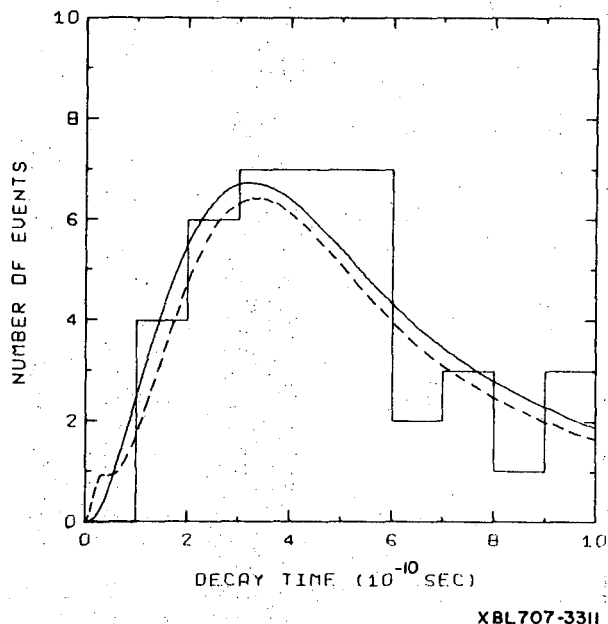


Fig. 1

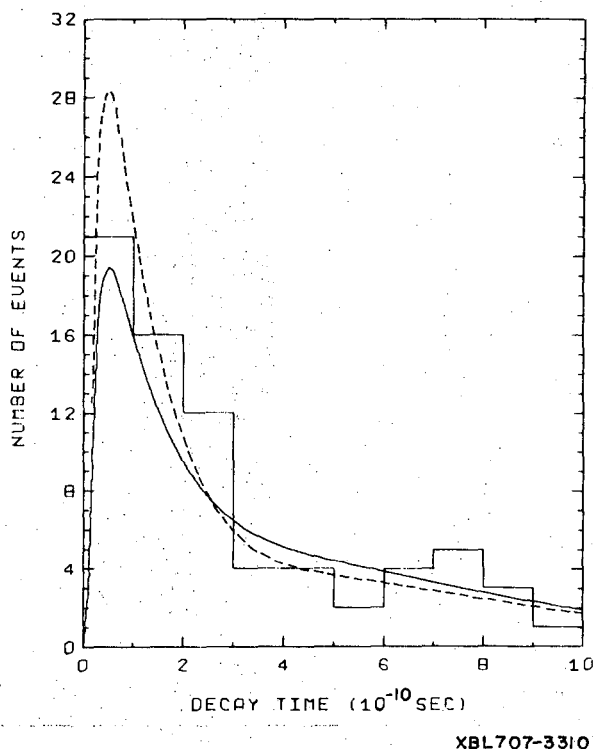


Fig. 2.

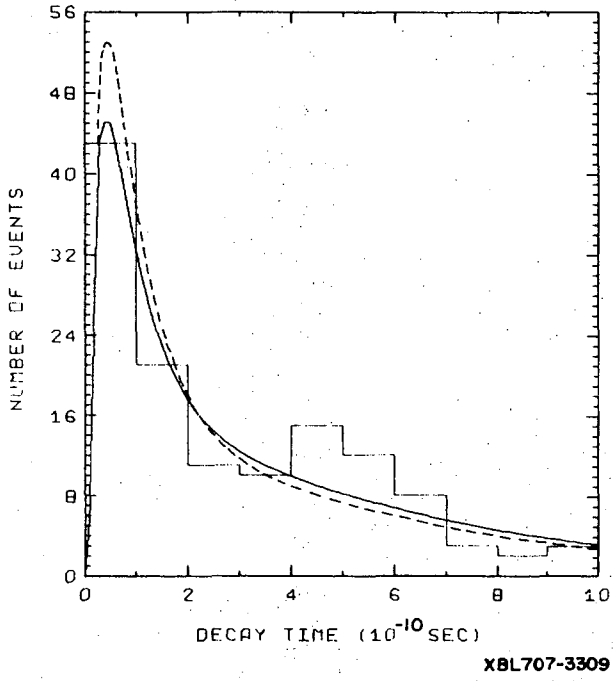


Fig. 3

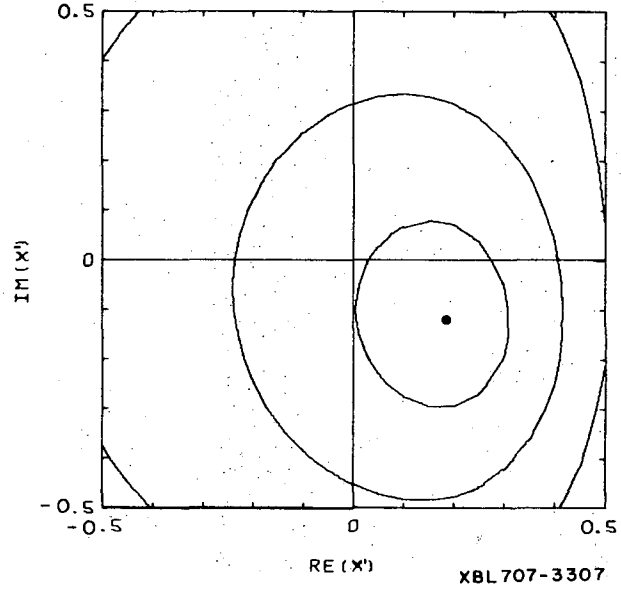


Fig. 5

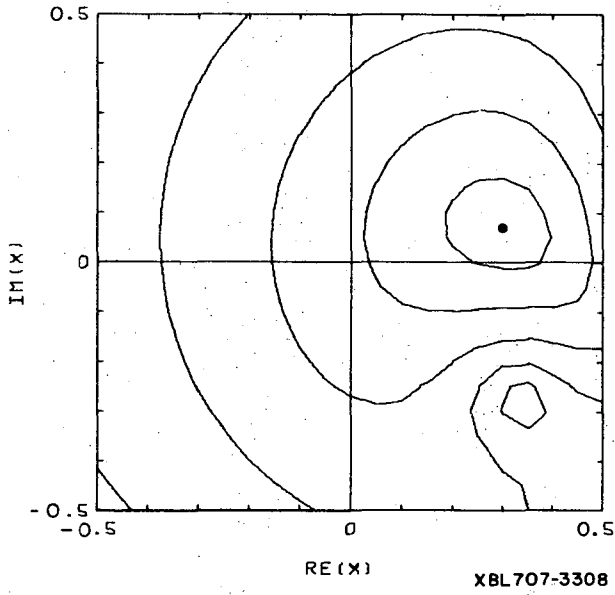


Fig. 4

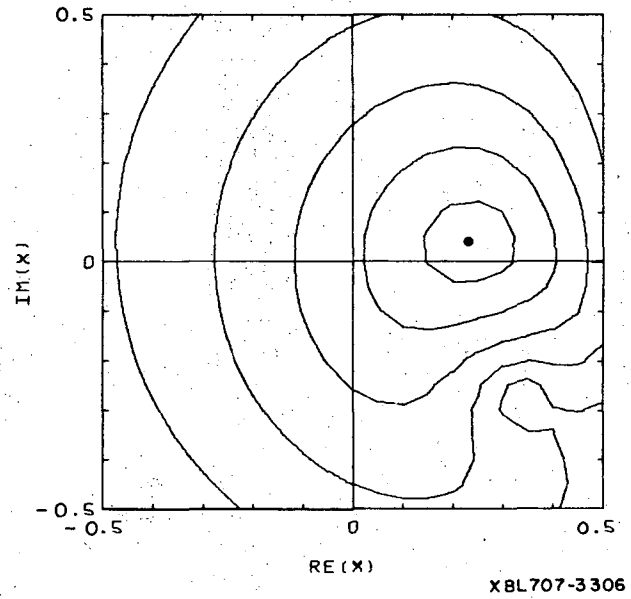


Fig. 6

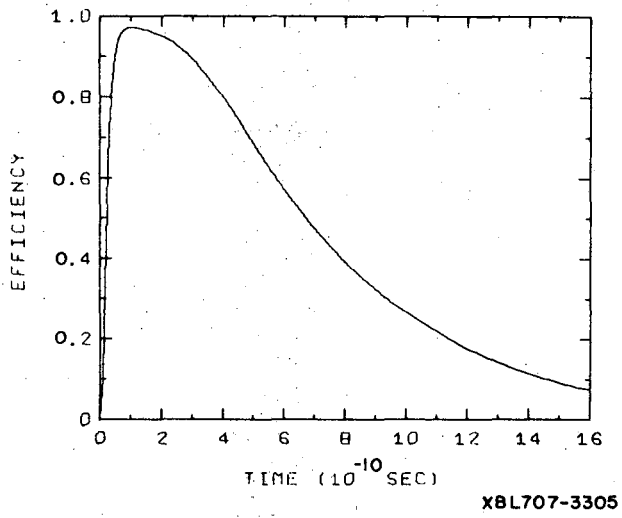


Fig. 7

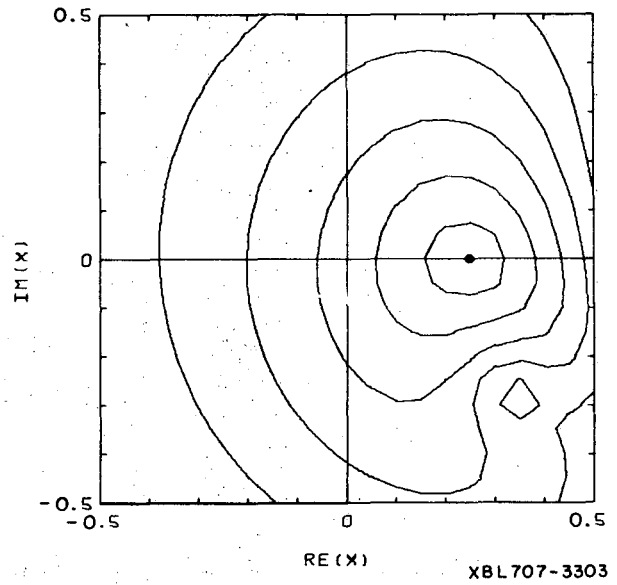


Fig. 9

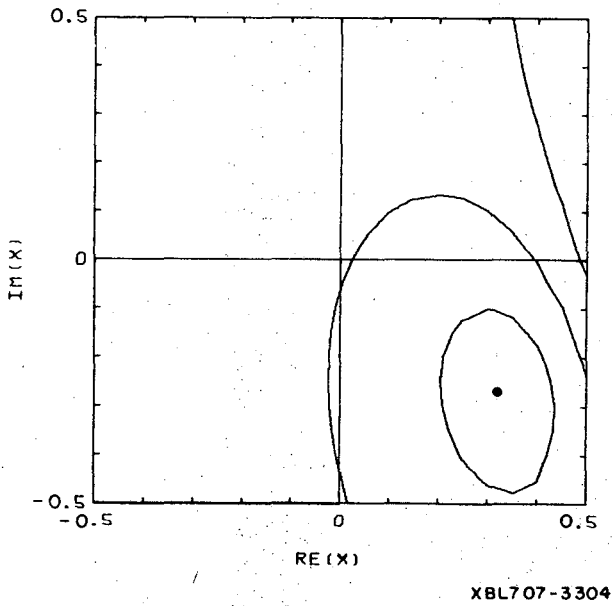


Fig. 8

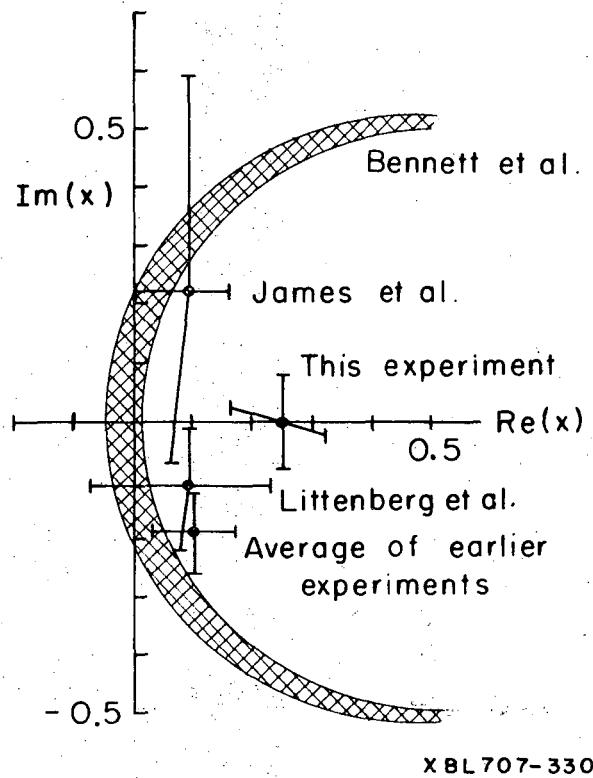


Fig. 10

LEGAL NOTICE

This report was prepared as an account of Government sponsored work. Neither the United States, nor the Commission, nor any person acting on behalf of the Commission:

- A. Makes any warranty or representation, expressed or implied, with respect to the accuracy, completeness, or usefulness of the information contained in this report, or that the use of any information, apparatus, method, or process disclosed in this report may not infringe privately owned rights; or*
- B. Assumes any liabilities with respect to the use of, or for damages resulting from the use of any information, apparatus, method, or process disclosed in this report.*

As used in the above, "person acting on behalf of the Commission" includes any employee or contractor of the Commission, or employee of such contractor, to the extent that such employee or contractor of the Commission, or employee of such contractor prepares, disseminates, or provides access to, any information pursuant to his employment or contract with the Commission, or his employment with such contractor.

TECHNICAL INFORMATION DIVISION
LAWRENCE RADIATION LABORATORY
UNIVERSITY OF CALIFORNIA
BERKELEY, CALIFORNIA 94720